Egyptian Society of Radiology and Nuclear Medicine

The Egyptian Journal of Radiology and Nuclear Medicine

www.elsevier.com/locate/ejrnm
www.sciencedirect.com

ORIGINAL ARTICLE

Triple negative breast cancer: MRI features in comparison to other breast cancer subtypes with correlation to prognostic pathologic factors

CrossMark

Noha Mohamed Osman [a],*, Nivine Chalabi [a], Nermine Mohamed Abd Raboh [b]

[a] *Department of Radiodiagnosis, Faculty of Medicine, Ain Shams University, Cairo, Egypt*
[b] *Department of Pathology, Faculty of Medicine, Ain Shams University, Cairo, Egypt*

Abstract *Objective:* This study aimed at determination of the MRI predictors of triple negative breast cancer (TNBC) in comparison to other breast cancer subtypes.

Materials and methods: The study retrospectively enrolled 185 female patients with 206 pathologically confirmed invasive breast cancers with different subtypes by immunohistochemistry. Histopathological analysis as well as MRI features of TNBC was compared to those of other breast cancer subtypes. MRI features included the tumor size, shape, margin, internal enhancement, intratumoral signal intensity on T2-WI, detectability by DW-MRI and ADC values.

Results: TNBCs showed higher histological grades ($p < 0.0001$) and younger patient age group ($p = 0.006$) compared to other tumor subtypes. At MRI, TNBCs were of larger size ($p < 0.0001$), round shape ($p < 0.0001$), smooth margin ($p < 0.0001$), with rim enhancement ($p < 0.0001$) and higher incidence of T2-WI tumoral hyperintensity ($p = 0.0002$) and intratumoral necrosis ($p < 0.0001$). No significant difference in tumor detectability was found by DW-MRI, however, TNBCs had higher ADC values ($p < 0.0001$).

Conclusion: In our study, TNBC patients were of younger age with higher grade malignancy. TNBC MRI predictors were unifocal rim enhancing mass with round shape, smooth margin, higher signal intensity on T2-WI, in addition to relatively larger sizes of tumors associated with high incidence of intratumoral necrosis and higher ADC values.

© 2014 The Egyptian Society of Radiology and Nuclear Medicine. Production and hosting by Elsevier B.V. Open access under CC BY-NC-ND license.

* Corresponding author. Address: 81 Mohy Eldeen Abdel Hameed, 8th District, Nasr City, Cairo, Egypt. Mobile: + 20 1001798342.
E-mail addresses: drnohaosman@yahoo.com (N.M. Osman), nivinechalabi@hotmail.com (N. Chalabi), nerminekortam@yahoo.com (N.M.A. Raboh).

1. Introduction

Triple negative breast cancer (TNBC) is defined by lack of expression of estrogen, progesterone and human epidermal growth factor receptor 2 (HER2) receptors (1). TNBC accounts for 11–20% of all subtypes of breast cancers (2,3), but accounts for 23–28% of locally advanced disease and

27% of breast cancers in African-American women (4,5). TNBC is characterized by distinct molecular, histopathological, and clinical features including a particularly aggressive clinical course and the lack of effective targeted therapies and hence unfavorable prognosis (6,7). Although TNBC has been extensively studied, there are few reports on the imaging features of TNBC (8).

Multiple studies have reported that endocrine therapy is not beneficial in treatment of TNBC, thus chemotherapy is currently the mainstay of systemic medical treatment. However, patients with TNBC have a worse outcome after chemotherapy than patients of other breast cancer subtypes (9).

Recently, analyses of gene expression profiles with cDNA microarray technology have segregated breast cancers into several subtypes with common molecular features: luminal A and B (both estrogen receptor (ER)-positive), basal-like (BL) and HER2-positive (all ER negative) (10–14). Approximately 70% of TN breast cancers are BL tumors. Currently, targeted therapy for breast cancer is guided in large part by the status of ER, PR and HER2, i.e., ER or PR for endocrine therapy and HER2 for anti-HER2 therapy. By immunohistochemistry, three major breast cancer subtypes are categorized: triple-negative (i.e., ER-, PR- and HER2-negative), HER2-positive (i.e., HER2-positive; ER and PR may be positive or negative), and ER-positive (i.e. ER positive, HER2-negative, PR may be positive or negative) types (15,16). These immunohistochemical subtypes correspond roughly to the molecular subtypes of basal-like, HER2-positive and luminal, respectively (17).

More than 90% of BL breast cancers and TNBCs present as invasive ductal carcinomas of no special type and are usually high-grade, demonstrate a high mitotic index, and contain central necrotic regions, pushing borders of invasion, and obvious lymphocytic infiltration (9,18).

TNBCs frequently present as palpable masses and may carry benign features on mammography and ultrasound imaging, which in turn may cause errors or delay in their accurate diagnosis. Consequently, mammography may be of limited value in screening patients who are at an increased risk of developing TNBC (8). Moreover, assessment of the palpable mass in core needle biopsy is less reliable than in excisional biopsy owing to smaller sample size or heterogeneous tumor status.

So, if it is possible to predict triple-negative breast cancer on the basis of imaging features particularly MRI characteristics, this additional information could assist in both pretreatment planning and prognosis.

This study was performed to determine the MRI predictors of triple negative invasive breast cancer (TNBC) on DCE-MRI and on DW-MRI in comparison to other breast cancer subtypes (ER-positive (ER+) and HER2-positive (HER2+) cancers.

2. Materials and methods

This study was conducted retrospectively in Ain Shams University Hospitals during the period from January 2012 to November 2013. We reviewed during this period all histopathologic and immunohistochemistry reports of patients whose core or excisional biopsies, breast conserving surgery, or mastectomy specimens were examined and proved to have invasive breast cancer, breast cancer subtype of each case was retrieved.

Of these patients, those who performed MRI breast before biopsy taking or pre-operative at our Radiology Department, their MRI examinations were recruited through the database system and were reinterpreted for multiple MRI parameters which were then correlated to the histopathologic report in an attempt to detect possible MRI imaging predictors differentiating TNBC from other breast cancer subtypes. Patients enrolled in our study performed MRI breast examination for variety of reasons including indeterminate mammographic and sonographic findings, accurately detecting the extent of disease, BIRADS (Breast Imaging Reporting and Data System) 3 or 4 masses in sonomammography with clinical suspicion of malignancy.

2.1. Patients

After reviewing the histopathology results, we identified 453 invasive breast cancers. We included in our study 206 breast cancers in 185 female patients aged 29 to 67 years (mean 48.2 years); 21 cases had bilateral breast cancer. Patients underwent MRI breast study at our Radiology Department before biopsy taking or pre-operative. We excluded the remaining 247 breast cancers of total identified 453 cancers for two reasons; 242 cancers in 242 patients did not have breast MRI examinations, in addition to 5 cancers in 5 patients, who had already started chemotherapy before the breast MRI examination, their exams were discarded for fear of change of tumor morphology. In patients with multifocal breast cancer, we selected the largest lesion in tumor analysis.

2.2. Breast MRI

All MRI examinations were performed with an Achieva; Philips Medical Systems, Bothell, WA, USA. All patients were examined in the prone position using a breast array coil. MRI protocol applied in our study was as follows: A survey sequence was followed by axial T1 and T2WI fast spin-echo sequence, axial and sagittal STIR fat suppressed images, single shot echo-planar DW imaging were obtained for both breasts prior to contrast administration, tri-directional diffusion gradients were used with b values: 0, 400 and 800 s/mm^2 to increase sensitivity to cellular packing, respiratory triggering was used for better resolution. Number of excitations was 2; matrix used was 256×256; and field of view of 34 cm; slice thickness was 3 mm and gap was 0. Dynamic contrast enhanced (DCE) sequence with axial and sagittal post-contrast T1WI fat suppressed images were taken after bolus injection of 0.1 mmol gadopentate dimeglumine per kilogram of body weight. The injection rate was 2 mL/s, followed by 20 mL saline flush. One acquisition was performed prior to contrast administration and three acquisitions were performed over a period of 6 min after intravenous contrast material injection.

At EasyVision; Philips Medical Systems workstation, ADC values were measured and time signal intensity curves were generated. The ADC values for the different b-values were obtained by placing 4 regions of interest (ROIs) on the ADC map in the area with pathological enhancement. The (ROI) area was between 1 and 2 cm^2, the final ADC value was the average of the 4 measured values for each b-value. Time intensity curves were generated by drawing region of interest (ROI) at the area of maximum higher visual enhancement, care was

taken to avoid central cystic regions. Curve patterns were categorized into three types (persistent (continuous), plateau, or washout pattern).

2.3. Interpretation of MR imaging findings

Blinded to histopathologic and immunohistochemistry results, the consultant radiologist with women's imaging subspecialty reviewed each breast MRI examination for the targeted breast lesion using the Breast Imaging Reporting and Data System (BIRADS) MR lexicon (19) with respect to: its location, morphology, visual evaluation of signal intensity in fat suppressed T2WI. Signal intensity on fat suppressed T2WI was determined as lower than, equivalent to, or higher than that of the surrounding breast tissue, its signal in DWI and corresponding ADC value and enhancement pattern with analysis of time/signal intensity curves.

3. Histopathology and immunohistochemistry

3.1. Technique

Pathologic reports from core needle, excisional biopsies, breast conserving surgery or mastectomy specimens were reviewed to identify invasive breast cancers with determination of the following prognostic factors: histologic grade and tumor subtype. Histologic grading was performed by the Elston–Ellis method (20), in which tubule formation, pleomorphism, and mitotic counts are scored 1–3 points. Cases scored within 3–5 ranged as grade 1, within 6–7 as grade 2, and within 8–9 as grade 3, in addition, necrosis within the tumor was recorded. Tissue sections which were Formalin-fixed and paraffin-embedded tissue were immunohistochemically stained with appropriate antibodies for ER (Dako, Carpinteria, CA, USA), PR (Dako, Carpinteria, CA, USA) and HER2 (Dako, CA, USA). Avidin Biotin immunoperoxidase complex technique was used by applying the super sensitive detection kit (Biogenex, CA, USA). The prepared tissue sections were fixed on poly-L-lysine coated slides overnight at 37 °C. They were deparaffinized in xylene, and rehydrated in graded alcohol series. Endogenous peroxidase activity was inhibited by immersing the sections in 3% methanol hydrogen peroxide for 10 min. Antigen retrieval was performed in a 20-mmol/L concentration of citrate buffer (pH 6.0) for 10 min. The sections were incubated for 2 h at room temperature, with the primary antibody. Biotinylated antimouse immunoglobulin and streptavidin conjugated to horseradish peroxidase were then added. Finally, 3,3-diaminobenzidine as the substrate or chromogen was used to form an insoluble brown product. The slides were counterstained with hematoxylin (DAKO) and coverslipped using a non aqueous mounting medium.

3.2. Interpretation

The status of each receptor was considered to be negative if the expression was less than 10% and positive if the expression was 10% or greater. The HER2 expression was semiquantitatively assessed as follows: 0 for no membranous staining, 1 + for weak uneven membranous staining in some of the tumor cells, 2 + for weak to moderate membranous staining in a large number of tumor cells, and 3 + for strong and complete membranous staining in almost all of the tumor cells.

4. Statistical analysis

To compare the MR imaging findings between TNBC, ER + and HER2 + breast cancers, we used $x2$ for categorical variables and ANOVA test for comparison of mean values or single variable. All analyses were performed by using software (SPSS, version 11.0; SPSS, Chicago, Ill), $p < 0.05$ is considered to indicate a significant difference.

5. Results

This study included 206 invasive breast cancers in 185 female patients, 42/206 (20.4%) were TNBC, 98/206 (47.6%) were ER + and 66/206 (32.0%) were HER2 + . Younger patients' age was detected in TNBC (mean value = 43.1 ± 8.2, $p = 0.006$) compared to ER + (45 ± 6.1) and HER2 + (47.4 ± 6.6) (Table 1). All breast cancer histological types were as follows: invasive ductal carcinoma (IDC) ($n = 186$), invasive lobular carcinoma (ILC) ($n = 6$), mucinous carcinoma ($n = 6$), medullary carcinoma ($n = 6$) and metaplastic carcinoma ($n = 2$) (Table 1). Regarding the results comparing pathological variables among the three tumor subtypes (Table 1), tumor histological grade was significantly different among tumor subtypes ($p < 0.0001$). The percentage of histological grade 3 (Fig. 1f) in TNBC (26/42, 61.9%) was higher than that of ER + (17/98, 17.3%) or HER2 + (21/66, 31.8%). Regarding MRI features (Table 2); all tumors were detected as areas of abnormal enhancement. The majority of lesions in all tumor subtypes showed mass like enhancement (36/42, 85.7% vs. 90/98, 91.8% and 63/66, 95.6% for TNBC, ER + and HER2 +, respectively) ($p = 0.199$). On DCE-MRI, larger tumor size was found in TNBC subtype ($p < 0.0001$) (25.4 ± 4.1 mm in TNBC vs. 19.8 ± 3.8 mm and 24.7 ± 5.2 mm in ER + and HER2 +, respectively). Most of tumors in the three subtypes were unifocal lesions ($p = 0.256$). The majority of TNBC subtype with mass like enhancement had round shape (24/42, 66.7%) ($p < 0.0001$) (Fig. 1), while 75/98, 83.3% and 52/66, 82.5% of ER + and HER2 + subtypes had irregular shapes (Figs. 2 and 3). The margins of TNBCs were most frequently smooth (26/42, 72.2%) ($p < 0.0001$) (Fig. 1), while in ER + and HER2 + margins were mostly spiculated (Fig. 3) in 60/98, 66.6% and 46/66, 73.0%, respectively. Intratumoral necrosis was found in 32/42, 76.2% of TNBCs (Fig. 1) versus 29/98, 29.6% and 15/66, 22.7% in ER + and HER2 + subtypes. The predominant internal enhancement pattern of the TNBCs was rim enhancement (Fig. 1) identified in 22/42, 61.1% ($p < 0.0001$), while heterogenous internal enhancement was the predominant in ER + (Fig. 2) and HER2 + (Fig. 3) subtypes, 65/98, 74.5% and 54/66, 85.7%, respectively. No statistically significant difference was found regarding the distribution and internal enhancement of non mass like cancers among the three tumor subtypes ($p = 0.554$ and 0.425, respectively). Intratumoral high signal intensity with respect to the surrounding breast tissue on unenhanced fat suppressed T2-weighted images was identified in 30/42, 71.4% of TNBCs (Fig. 1) which corresponded morphologically and pathologically to intratumoral necrosis, compared to 38/98, 38.8%

Table 1 Histopathologic data of patients with TN, ER+ and HER2+ breast cancer subtypes.

Histopathological features	Tumor subtype			
	TN (42 tumors)	ER+ (98 tumors)	HER2+ (66 tumors)	p value
Patients' age (mean)	43.1 ± 8.2	45 ± 6.1	47.4 ± 6.6	0.006
Histological grade				<0.0001
1 (low)	4 (9.5%)	52 (53.1%)	10 (15.1%)	
2 (moderate)	12 (28.6%)	29 (25.6%)	35 (53.0%)	
3 (high)	26 (61.9%)	17 (17.3%)	21 (31.8%)	
Histological type				0.0733
IDC (NOS)	36 (85.7%)	92 (93.9%)	58 (87.9%)	
ILC	1 (2.4%)	4 (4.1%)	1 (1.5%)	
Medullary	2 (4.8%)	0	4 (6.1%)	
Metaplastic	0	0	2 (3.0%)	
Mucinous	3 (7.1%)	2 (2.0%)	1 (1.5%)	

Abbreviations: TN = triple negative; ER = estrogen receptor; HER2 = human epidermal growth factor receptor; IDC = invasive ductal carcinoma; NOS = not otherwise specified; ILC = invasive lobular carcinoma.
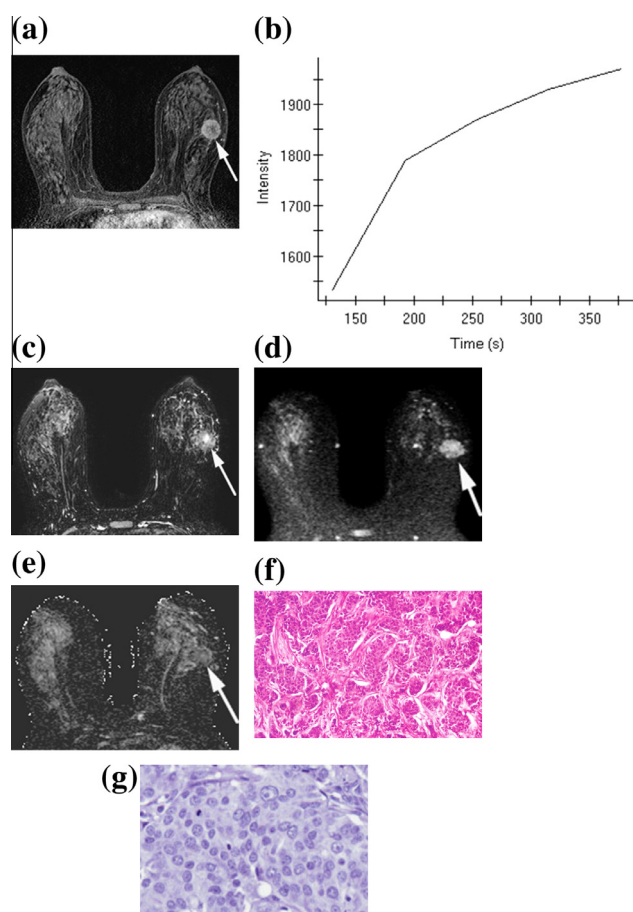

Figure 1 TNBC IDC of the left breast in 33-year old-female. (a) Axial contrast enhanced T1-WI with fat suppression showing left breast 31.5 mm round mass with smooth margin and rim enhancement pattern (arrow). (b) Time signal intensity curve shows initial rise then persistent (continuous) pattern. (c) Axial fat suppressed T2-WI indicates very high central signal intensity corresponding to intratumoral necrosis (arrow). (d and e) DWI and ADC map respectively showing peripheral restricted diffusion and low ADC (arrowed) (mean ADC value was $1.102 \times 10^{-3} \pm 0.111$). (f) H and E stain showing grade 3 IDC with solid infiltrating masses of malignant cells. (g) Negative ER immunostaining.

and 22/66, 33.4% in ER+ and HER2+ subtypes ($p = 0.0002$). Time intensity analysis revealed type III (washout) and type II (plateau) curves in 26/42, 61.9% of TNBC compared to 92/98, 93.8% and 64/66, 97.0% in ER+ and HER2+, respectively ($p < 0.0001$) (Figs. 2 and 3), while 16/42, 38.1% of TNBCs showed type I persistent (continuous) curve (Fig. 1). Visual delectability of the three tumor subtypes at DWI was not significantly different among tumor subtypes. ADC values were significantly different among tumor subtypes ($p < 0.0001$), the mean ADC value of TNBC was 1.097×10^{-3} mm^2/s which was higher than that of ER+ (0.620×10^{-3} mm^2/s) or HER2+ (0.632×10^{-3} mm^2/s).

6. Discussion

TNBC has been studied extensively in the oncology and pathology literature; however, few reports are available describing its imaging features. Current literature suggests that imaging features of TNBC are significantly different from other primary breast cancer immunotypes [8].

Similar to previous reports [9,18,21–26], our study results showed that TNBCs were associated with younger patients' age (mean; 43.1 years, $p = 0.006$), high tumor grades (26/42, 61.9% grade 3, $p < 0.0001$) but no statistically significant difference was found between the histologic types of TNBC and the other subtypes. IDC (NOS) was the predominant histological type (36/42, 85.7%, $p = 0.073$).

In the current literature, DCE-MRI most significant features associated with TNBCs were: round or oval shape [22,24,27], smooth mass margin [22–25,27], rim type of internal enhancement [22–24,27–29], high signal intensity on fat suppressed T2-weighted images (T2-WI) [22,23,25,30] and higher ADC values [22,31–33]. Other contradictory features were: unifocal lesion [23–25,30], larger size of tumor mass [21,22,25,26,30] and malignant type time signal intensity curves (wash out or plateau) [22–25,27,30]. In our study, TNBCs showed many features in DCE-MRI which were in concordance with the previously mentioned results, which were unifocality of tumors (37/42, 88.1%, $p = 0.2567$), round shape (24/42, 66.7%, $p < 0.0001$), smooth mass margin (26/42, 72.2%, $p < 0.0001$), TNBCs had the largest tumor size (25.4 ± 4.1, $p < 0.0001$), rim enhancement (22/42, 61.1%, $p < 0.0001$) and higher ADC values (mean 1.097 ± 203.9,

Table 2 MRI features of TN, ER+ and HER2+ breast cancer subtypes.

MRI parameters	Tumor subtype			p value
	TN (42 tumors)	ER+ (98 tumors)	HER2+ (66 tumors)	
T2-WI signal intensity				0.0002
Low/equal	12 (28.6%)	60 (61.2%)	44 (66.6%)	
High/very high	30 (71.4%)	38 (38.8%)	22 (33.4%)	
DCE-MRI				
Tumor size (mm)	25.4 ± 4.1	19.8 ± 3.8	24.7 ± 5.2	<0.0001
Multifocality				0.2567
Yes	5 (11.9%)	14 (14.3%)	4 (6.1%)	
No	37 (88.1%)	84 (85.7%)	62 (93.9%)	
Presence of intratumoral necrosis				<0.0001
Yes	32 (76.2%)	29 (29.6%)	15 (22.7%)	
No	10 (23.8%)	69 (70.4%)	51 (77.3%)	
Morphology				0.199
Mass	36 (85.7%)	90 (91.8%)	63 (95.6%)	
Non mass	6 (14.3%)	8 (8.2%)	3 (4.5%)	
Mass				
Shape				<0.0001
Round	24 (66.7%)	10 (11.1%)	6 (9.5%)	
Oval	3 (8.3%)	5 (5.6%)	2 (3.2%)	
Lobular	1 (2.8%)	0	3 (4.8%)	
Irregular	8 (22.2%)	75 (83.3%)	52 (82.5%)	
Margin				<0.0001
Smooth	26 (72.2%)	0	0	
Irregular	7 (19.4%)	30 (33.3%)	15 (27.0%)	
Spiculated	3 (8.4%)	60 (66.7%)	46 (73.0%)	
Internal enhancement				<0.0001
Homogenous	5 (13.9%)	18 (20.0%)	6 (9.5%)	
Heterogenous	9 (25.0%)	65 (74.5%)	54 (85.7%)	
Rim	22 (61.1%)	7 (7.1%)	3 (4.8%)	
Non mass				
Distribution				0.554
Focal	0	0	0	
Linear	0	1 (12.5%)	0	
Ductal	0	0	1 (33.3%)	
Segmental	4 (66.7%)	3 (37.5%)	1 (33.3%)	
Regional	2 (33.3%)	4 (50.0%)	1 (33.3%)	
Internal enhancement				0.425
Homogenous	3 (50.0%)	4 (50.0%)	1 (33.3%)	
Heterogenous	2 (33.3%)	1 (37.5%)	2 (66.7%)	
Clumped	1 (16.7%)	3 (12.5%)	0	
Kinetic curves				<0.0001
I (persistent)	16 (38.1%)	6 (6.1%)	2 (3.0%)	
II (plateau)	7 (16.7%)	7 (7.1%)	4 (6.1%)	
III (wash out)	19 (45.2%)	85 (86.7%)	60 (90.9%)	
DW-MRI				
ADC (mean value × 10^{-3} mm^2/s)	1.097×10^{-3} ± 0.203	0.620×10^{-3} ± 0.148	0.632×10^{-3} ± 0.162	<0.0001

Abbreviations: TN = triple negative; ER = estrogen receptor; HER2 = human epidermal growth factor receptor; DCE = dynamic contrast enhanced magnetic resonance imaging; DW = diffusion weighted; ADC = apparent diffusion coefficient.

$p < 0.0001$) than other breast cancer subtypes in this study. Most of breast cancer subtypes including TNBCs in this study showed malignant pattern kinetic curves (type II and III), however a significant difference was found between the 3 tumor subtypes ($p < 0.0001$) as 16/42, 38.1% of TNBCs showed persistent (type I) kinetic curves, this may be

attributed to non homogenous tumor enhancement which was also declared by Uematsu et al. (23) who found that TNBCs in their study had predominant persistent (continuous) pattern curves ($p = 0.005$) (23).

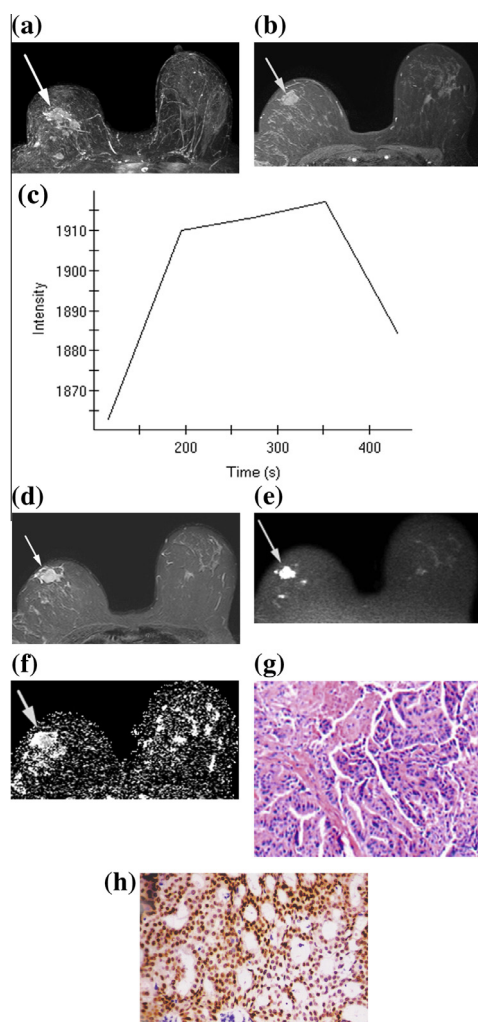Putti et al. (34) resulted in their study that TNBCs were characterized morphologically by high grade, smooth margin

Figure 2 Recurrent ER+ IDC of the right breast in a 53-year-old female after conservative breast surgery (lumpectomy). (a) MIP shows multifocal pattern of recurrence (arrow). (b) Axial contrast enhanced T1-WI with fat suppression showing the largest mass measuring 21.5×23.1 mm, irregular in shape with irregular margin and heterogenous enhancement (arrow). (c) Time intensity curve indicates rapid initial rise then wash out pattern. (d) Axial fat suppressed T2-WI showing high signal of the mass (arrow). (e and f) DWI and ADC map respectively showing restricted diffusion and low ADC (arrowed) (mean ADC value was $0.823 \times 10^{-3} \pm 0.106$). (g) H and E stain showing grade 2 IDC with sheets and tubules of malignant cells. (g) Strong nuclear positivity for ER immunostaining.

and central necrosis. This is consistent with our TNBC group in which MRI revealed intratumoral necrosis in 32/42, 76.2% ($p < 0.0001$) (Table 2) of TNBC groups compared to 29/98, 29.6% and 15/66, 22.7% in ER+ and HER2+ subtypes respectively. All intratumoral necrosis were proven by histopathological analysis.

In this study, 90 of 206 breast cancers showed signal hyperintensity on fat suppressed T2-weighted images, 30 tumors were TNBC representing 71.4% of TNBC group ($p = 0.0002$) (Table 2). Twenty seven of 30 TNBCs with high signal in fat suppressed T2-weighted images had intratumoral central necrosis while 3 tumors were hyperintense without
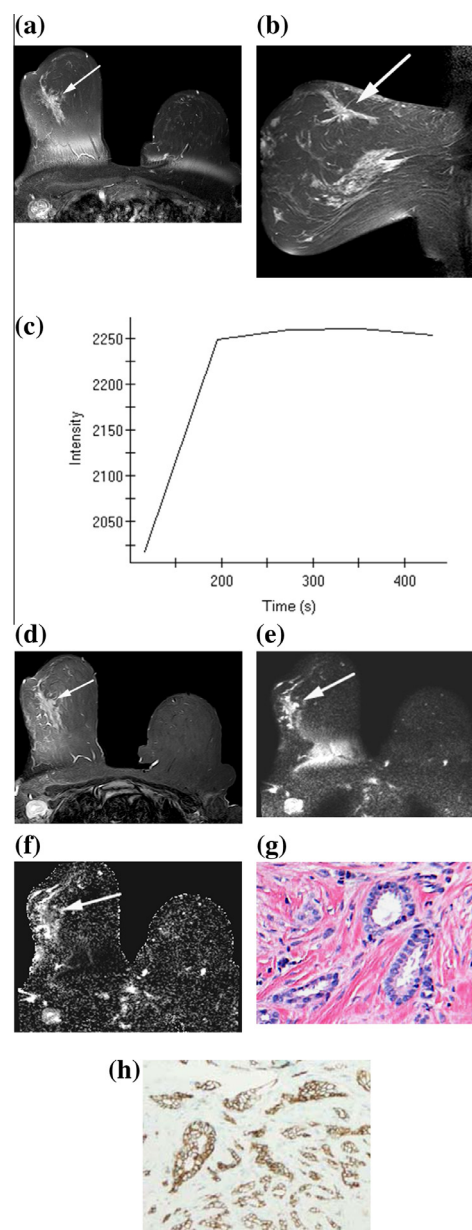

Figure 3 HER2+ IDC of the right breast in a 41-year-old female. (a and b) Axial and sagittal contrast enhanced T1-WI with fat suppression showing an irregular 34.3×20.4 mm spiculated mass (arrow). (b) Time intensity curve shows initial rise followed by plateau pattern. (c) Axial T2-WI with fat suppression showing isointense signal of the mass (arrow) to the surrounding breast tissue. (d and e) DWI and ADC map respectively showing restricted diffusion and low ADC (arrowed) (mean ADC value was $0.734 \times 10^{-3} \pm 0.109$). (g) H and E showing grade 1 IDC with angulated tubules and cellular stroma. (h) Positive HER2 immunostaining (2+) with moderate complete membranous staining in large number of the tumor cells.

necrosis; their histopathology analysis revealed that they were mucinous carcinomas. We could correlate the hyperintensity in fat suppressed T2-WI in our study to the central necrosis in most of the cases. This result could be supported by the finding that in all 27 cases, areas of tumor necrosis showed no

restriction at DW-MRI and ADC map with corresponding high ADC values. These results were concordant with Uematsu et al. (23) and Metz et al. (35), who resulted in their studies that intratumoral necrosis correlated to hyperintensity on T2-WI ($p < 0.001$) and was significantly associated with TNBCs (23). In addition, Youk et al. (22) and Uematsu et al. (23) found that areas of tumor necrosis showed a significant correlation with increased diffusion and higher ADC values on DWI and was found more frequently in cases of TNBC. Another explanation for increased ADC value in TNBCs was reported by Ludovini et al. and kim et al. (32,36) who stated that in ER+ tumors, the ADC value becomes less than in ER–as the estrogen receptors inhibit the tumor angiogenesis decreasing perfusion and thus affecting the ADC value.

In our study, rim internal enhancement was predominant in TNBCs (22/42, 61.1%, $p < 0.0001$) (Table 2), this may be due to tumor necrosis compared to predominant heterogenous internal enhancement in the other subtypes. Our results are consistent with many studies (22–24,27–29). Teifke et al. (30) declared that rim enhancement is the most useful MR feature for identifying TNBC. Rim enhancement is associated with higher grade tumors (37,38) and tends to predict an unfavorable prognosis for malignant lesions especially those with smooth margins (36). It is observed that rim enhancing masses with a smooth margin are typical features of masses associated with triple-negative breast cancer (23).

No statistical significance was found between breast cancer tumor subtypes as regards the mass type lesion where all tumor subtypes were predominantly of mass type ($p = 0.199$) (Table 2), this was concordant with many reports (21,24,25,27,30), the distribution and internal enhancement patterns of the non mass type of tumors ($p = 0.554$ and $p = 0.425$, respectively) (Table 2), similar results were found by Youk et al. (22) and Choi et al. (31) as well as regarding the visual detectability of tumors at DW-MRI, similar results were found by Youk et al. (22).

In conclusion, our study resulted that TNBC patients were of younger age with higher grade malignancy. TNBC presented several MRI predictors on DCE-MRI such as unifocal rim enhancing mass with round shape, smooth margin, higher signal intensity on fat suppressed T2-WI, in addition to relatively larger size of tumors associated with high incidence of intratumoral necrosis and higher ADC values on DWI. These features could be beneficial in identifying TNBC from ER+ and HER2+ breast cancer subtypes.

Source of funding

None declared.

Conflicts of interest

None declared.

References

(1) Brenton JD, Carey LA, Ahmed AA, Caldas C. Molecular classification and molecular forecasting of breast cancer: ready for clinical application? J Clin Oncol 2005;23(29):7350–60.

(2) Rakha EA, El-Sayed ME, Green AR, Lee AH, Robertson JF, Ellis IO. Prognostic markers in triple-negative breast cancer. Cancer 2007;109:25–32.

(3) Lin NU, Vanderplas A, Hughes ME, Theriault RL, Edge SB, Wong Y. Clinicopathological features and sites of recurrence according to breast cancer subtype in the National Comprehensive Cancer Network (NCCN). J Clin Oncol 2009;27, 15s: Abstr 543.

(4) Dolle JM, Daling JR, White E, Brinton LA, Doody DR, Porter PL, et al. Risk factors for triple-negative breast cancer in women under the age of 45 years. Cancer Epidemiol Biomarkers Prev 2009;18:1157–66.

(5) Millikan R, Newman B, Tse CK, Moorman PG, Conway K, Dressler LG, et al. Epidemiology of basal-like breast cancer. Breast Cancer Res Treat 2008;109:123.

(6) Gluz O, Liedtke C, Gottschalk N, Pusztai L, Nitz U, Harbeck N. Triple-negative breast cancer—current status and future directions. Ann Oncol 2009;20(12):1913–27.

(7) Podo F, Buydens LM, Degani H, Hilhorst R, Klipp E, Gribbestad IS, et al. Triple-negative breast cancer: present challenges and new perspectives. Mol Oncol 2010;4:209–29.

(8) Dogan BE, Turnbull LW. Imaging of triple-negative breast cancer. Ann Oncol 2012;23(Suppl 6), vi23-9.

(9) Fulford LG, Easton DF, Reis-Filho JS, Sofronis A, Gillett CE, Lakhani SR, et al. Specific morphological features predictive for the basal phenotype in grade 3 invasive ductal carcinoma of breast. Histopathology 2006;49(1):22–34.

(10) Montagna E, Bagnardi V, Rotmensz N, Viale G, Cancello G, Mazza M, et al. Immunohistochemically defined subtypes and outcome in occult breast carcinoma with axillary presentation. Breast Cancer Res Treat 2011;129:867–75.

(11) Sorlie T, Perou CM, Tibshirani R, Aas T, Geisler S, Johnsen H, et al. Gene expression patterns of breast carcinomas distinguish tumor subclasses with clinical implications. Proc Natl Acad Sci USA 2001;98:10869–74.

(12) Perou CM, Sorlie T, Eisen MB, van de Rijn M, Jeffrey SS, Rees CA, et al. Molecular portraits of human breast tumours. Nature 2000;406:747–52.

(13) Li SP, Padhani AR, Taylor NJ, Beresford MJ, Ah-See ML, Stirling JJ, et al. Vascular characterization of triple negative breast carcinomas using dynamic MRI. Eur Radiol 2011;21:1364–73.

(14) van de Vijver MJ, He YD, van't Veer LJ, Dai H, Hart AA, Voskuil DW, et al. A gene expression signature as a predictor of survival in breast cancer. N Engl J Med 2002;347:1999–2009.

(15) Desmedt C, Haibe-Kains B, Wirapati P, Buyse M, Larsimont D, Bontempi G, et al. Biological processes associated with breast cancer clinical outcome depend on the molecular subtypes. Clin Cancer Res 2008;14:5158–65.

(16) Sanchez-Munoz A, Garcia-Tapiador AM, Martinez-Ortega E, Dueñas-García R, Jaén-Morago A, Ortega-Granados AL, et al. Tumour molecular subtyping according to hormone receptors and HER2 status defines different pathological complete response to neoadjuvant chemotherapy in patients with locally advanced breast cancer. Clin Transl Oncol 2008;10:646–53.

(17) De Ronde JJ, Hannemann J, Halfwerk H, Mulder L, Straver ME, Vrancken Peeters MJ, et al. Concordance of clinical and molecular breast cancer subtyping in the context of preoperative chemotherapy response. Breast Cancer Res Treat 2010;119:119–26.

(18) Livasy CA, Karaca G, Nanda R, Tretiakova MS, Olopade OI, Moore DT, et al. Phenotypic evaluation of the basal-like subtype of invasive breast carcinoma. Mod Pathol 2006;19(2):264–71.

(19) American College of Radiology. Breast imaging reporting and data system (BI-RADS). 4th ed. Reston, Va: American College of Radiology, 2003.

(20) Elston CW, Ellis IO. Pathological prognostic factors in breast cancer. The value of histological grade in breast cancer: experience from a large study with long-term follow-up. Histopathology 1991;19:403–10.

(21) Ko ES, Lee BH, Kim HA, Noh WC, Kim MS, Lee SA. Triple-negative breast cancer: correlation between imaging and pathological findings. Eur Radiol 2010;20:1111–7.

(22) Youk JH, Son EJ, Chung J, Kim JA, Kim EK. Triple-negative invasive breast cancer on dynamic contrast-enhanced and diffusion-weighted MR imaging: comparison with other breast cancer subtypes. Eur Radiol 2012;22(8):1724–34.

(23) Uematsu T, Kasami M, Yuen S. Triple-negative breast cancer: correlation between MRI imaging and pathologic findings. Radiology 2009;250:638–47.

(24) Costantini M, Belli P, Distefano D, Bufi E, Di Matteo M, Rinaldi P, et al. Magnetic resonance imaging features in Triple-Negative Breast Cancer: comparison with luminal and HER2- overexpressing tumors. Clin Breast Cancer 2012;12(5):331–9.

(25) Sung JS, Jochelson MS, Brennan S, Joo S, Wen YH, Moskowitz C, et al. MR imaging features of triple-negative breast cancers. Breast J 2013;19(6):643–9.

(26) Li SP, Padhani AR, Taylor NJ, Beresford MJ, Ah-See ML, Stirling JJ, et al. Vascular characterisation of triple negative breast carcinomas using dynamic MRI. Eur Radiol 2011;21(7):1364–73.

(27) Dogan BE, Gonzalez-Angulo AM, Gilcrease M, Dryden MJ, Yang WT. Multimodality imaging of triple receptor-negative tumors with mammography, ultrasound, and MRI. AJR Am J Roentgenol 2010;194(4):1160–6.

(28) Boisserie-Lacroix M, Macgrogan G, Debled M, Ferron S, Asad-Syed M, McKelvie- Sebileau P, et al. Triple-negative breast cancers: associations between imaging and pathological findings for triple-negative tumors compared with hormone receptor-positive/human epidermal growth factor receptor-2-negative breast cancers. Oncologist 2013;18(7):802–11.

(29) Teifke A, Behr O, Schmidt M, Victor A, Vomweg TW, Thelen M, et al. Dynamic MR imaging of breast lesions: correlation with microvessel distribution pattern and histologic characteristics of prognosis Dynamic MR imaging of breast lesions: correlation with microvessel distribution pattern and histologic characteristics of prognosis. Radiology 2006;239(2):351–60.

(30) Chen JH, Agrawal G, Feig B, Baek HM, Carpenter PM, Mehta RS, et al. Triple negative breast cancer: MRI features in 29 patients. Ann Oncol 2007;18(12):2042–3.

(31) Choi SY, Chang YW, Park HJ, Kim HJ, Hong SS, Seo DY. Correlation of the apparent diffusion coefficiency values on diffusion-weighted imaging with prognostic factors for breast cancer. Br J Radiol 2012 Aug;85(1016):e474–9.

(32) Kim SH, Cha ES, Kim HS, Kang BJ, Choi JJ, Jung JH, et al. Diffusion-Weighted Imaging of Breast Cancer: Correlation of the Apparent Diffusion Coefficient Value with Prognostic Factors. J Magn Reson Imaging 2009;30(3):615–20.

(33) Martincich L, Deantoni V, Bertotto I, Redana S, Kubatzki F, Sarotto I, et al. Correlations between diffusion-weighted imaging and breast cancer biomarkers. Eur Radiol 2012;22(7):1519–28.

(34) Putti TC, El-Rehim DM, Rakha EA, Paish CE, Lee AH, Pinder SE, et al. Estrogen receptor-negative breast carcinomas: a review of morphology and immunophenotypical analysis. Mod Pathol 2005;18:26–35.

(35) Metz S, Daldrup-Link HE, Richter T, Räth C, Ebert W, Settles M, et al. Detection and quantification of breast tumor necrosis with MR imaging: value of the necrosis- avid contrast agent Gadophrin-3. Acad Radiol 2003;10:484–90.

(36) Ludovini V, Sidoni A, Pistolal L, Bellezza G, De Angelis V, Gori S, et al. Evaluation of the prognostic role of vascular endothelial growth factor and microvessel density in stages I and II breast cancer patients. Breast Cancer Res Treat 2003;81:159–68.

(37) Szabó BK, Aspelin P, Kristoffersen Wiberg M, Tot T, Boné B. Invasive breast cancer: correlation of dynamic MRI features with prognostic factors. Eur Radiol 2003;13:2425–35.

(38) Lee SH, Cho N, Kim SJ, Cha JH, Cho KS, Ko ES, et al. Correlation between high resolution dynamic MRI features and prognostic factors in breast cancer. Korean J Radiol 2008;9:10–8.